Automatic Parameterization Strategy for Cardiac Electrophysiology Simulations

Caroline Mendonca Costa[1], Elena Hoetzl[1], Bernardo Martins Rocha[2], Anton J Prassl[1], Gernot Plank[1,3]

[1]Institute of Biophysics, Medical University of Graz, Graz, Austria
[2]Department of Computer Science, Universidade Federal de Juiz de Fora, Juiz de Fora, Brazil
[3]Oxford e-Research Centre, University of Oxford, Oxford, UK

Abstract

Driven by recent advances in medical imaging, image segmentation and numerical techniques, computer models of ventricular electrophysiology account for increasingly finer levels of anatomical and biophysical detail. However, considering the large number of model parameters involved parameterization poses a major challenge. A minimum requirement in combined experimental and modeling studies is to achieve good agreement in activation and repolarization sequences between model and experiment or patient data. In this study, we propose basic techniques which aid in determining bidomain parameters to match activation sequences. An iterative parameterization algorithm is implemented which determines appropriate bulk conductivities which yield prescribed velocities. In addition, a method is proposed for splitting the computed bulk conductivities into individual bidomain conductivities by prescribing anisotropy ratios.

1. Introduction

In-silico models of ventricular electrophysiology are widely recognized to be an invaluable adjunct to experimental in-vitro or in-vivo models. Recent advances in medical imaging, image segmentation and image-based finite element (FE) mesh generation [1], along with major advances in the numerical solution of model equations have led to the generation of micro-anatomically accurate and biophysically detailed ventricular models [2]. However, considering the large number of parameters in these models data assimilation and parameterization poses a major challenge.

A minimum requirement in such modeling studies which aim at making case-specific predictions on ventricular electrophysiology is that activation and repolarization sequences are carefully matched. Conduction velocity in the ventricles is orthotropic and may vary in space, thus profoundly influencing shape and location of activation isochrones. Moreover, while anisotropy ratios, on mathematical grounds, are of rather minor relevance when simulating impulse propagation in tissue, they play a prominent role when the stimulation of cardiac tissue via externally applied electric fields is studied.

In this study, we propose an automatic tuning procedure which iteratively refines bidomain bulk conductivities using observed conduction velocities in 1D cable simulations as input. We propose a method for splitting these bulk conductivities into individual bidomain conductivities by prescribing anisotropy ratios and using those experimental data afflicted with the smallest uncertainty.

2. Methods

2.1. Governing equations

The bidomain equations are considered to be among the most accurate descriptions of cardiac bioelectricity at a macroscopic size scale. In the elliptic-parabolic form they are given by

$$\begin{aligned} -\nabla \cdot (\boldsymbol{\sigma}_i + \boldsymbol{\sigma}_e) \nabla \phi_e &= \nabla \cdot \boldsymbol{\sigma}_i \nabla V_m \\ \beta C_m \frac{\partial V_m}{\partial t} &= \nabla \cdot \boldsymbol{\sigma}_i \nabla \phi_i - \beta I_{ion}(V_m, \boldsymbol{\eta}) \end{aligned} \quad (1)$$

where ϕ_i and ϕ_e are intra- and extracellular potentials, respectively, $V_m = \phi_i - \phi_e$ is the transmembrane voltage, $\boldsymbol{\sigma_i}$ and $\boldsymbol{\sigma_e}$ are the intra- and extracellular conductivity tensors, respectively, β is the membrane surface-to-volume ratio, C_m is the membrane capacitance per unit area, and I_{ion} is the membrane ionic current density which depends on V_m and a set of state variables, $\boldsymbol{\eta}$. At tissue boundaries, no flux boundary conditions are imposed on ϕ_i and ϕ_e.

In a 1D case where impulse propagation occurs along a thin strand of tissue aligned with an axis ζ, or in the case of a planar wave front moving along an axis ζ, the mon-

odomain equation

$$\beta C_m \frac{\partial V_m}{\partial t} = \nabla \cdot \sigma_{m\zeta} \nabla V_m - \beta I_{ion}(V_m, \boldsymbol{\eta}), \quad (2)$$

is equivalent to the bidomain equation if the monodomain conductivity $\sigma_{m\zeta}$ is chosen to be half the harmonic mean between intracellular and interstitial conductivities, that is,

$$\sigma_{m\zeta} = \frac{\sigma_{i\zeta}\sigma_{e\zeta}}{\sigma_{i\zeta} + \sigma_{e\zeta}}, \quad (3)$$

suggesting that conduction velocity in a full 3D bidomain model at a given location can be matched closely by an equivalent monodomain model using a harmonic mean conductivity tensor.

2.2. Conduction velocity parameterization

Conduction velocity, C^v, is not a parameter in the bidomain equations and as such cannot be directly parameterized. However, assuming a continuously propagating planar wavefront along a given direction, ζ, space and time are related by $\zeta = C^v_\zeta \cdot t$ which allows to replace spatial derivatives in Eq. (2) by temporal derivatives

$$\frac{\sigma_{m\zeta}}{\beta}\frac{\partial^2 V_m}{\partial \zeta^2} = \frac{\sigma_{m\zeta}}{C^{v2}\beta}\frac{\partial^2 V_m}{\partial t^2} = C_m \frac{\partial V_m}{\partial t} + I_{ion}(V_m, \boldsymbol{\eta}). \quad (4)$$

Since membrane properties on the right hand side remain unchanged, V_m remains to be a solution of Eq. (4) as long as $\sigma_{m\zeta}/C^{v2}/\beta$ is constant. Thus C^v is governed by the proportionality relation

$$C^v_\zeta \propto \sqrt{\sigma_{m\zeta}/\beta}. \quad (5)$$

Ideally, these parameters and their spatial variation would be measured accurately *in-vivo* for a given subject, however, this is difficult, if not impossible, to achieve. Even when considering *ex-vivo* measurements, the number of reports in the literature is scarce and the variation in measured values across these studies is vast. These uncertainties inevitably arise due to the significant degree of biological variation and the substantial errors in the measurement techniques themselves.

2.3. Iterative parameterization strategy

Modeling and technical uncertainties may also have an impact on model predictions as well. For instance, C^v also depends on the particular model used to describe cellular dynamics. Uncertainties due to technical factors such as discretization errors are of lesser concern since these are, in general, small (<5%) relative to the uncertainties in model parameters. Therefore, resorting to use overly expensive numerical schemes to minimize discretization errors is not a likely candidate strategy for improving the predictive power of computer simulations. The direct use of experimentally measured conductivity values, is not warranted neither when aiming to achieve good agreement with a specific experiment.

To find a balanced trade-off, we propose a strategy which relies on prescribing C^v directly. This is based on the consideration that C^v is a quantity which is much easier, more robustly and more accurately measurable in-vivo than tissue conductivities. The proposed strategy assumes that C^v predicted by a given computer simulation setup, $\bar{C}^v_\zeta$, can be represented as a function

$$\bar{C}^v_\zeta = \bar{C}^v_\zeta\left(\sigma_{m\zeta}, \beta, I_{ion}, \Delta\zeta, \xi\right). \quad (6)$$

which depends on the main factors conductivity along an axis ζ, $\sigma_{m\zeta}$, surface-to-volume ratio, β, the chosen model of cellular dynamics, I_{ion}, and technical factors such as spatial discretization, $\Delta\zeta$, and others such as the used spatio-temporal discretization method, convergence criteria and error tolerances, the influence of which shall be summarized by ξ. In most practical scenarios, ξ, I_{ion} and $\Delta\zeta$ are parameters defined by users in the course of selecting a simulation software, an ionic model and a provided mesh to describe the geometry. Thus, only two free parameters, $\sigma_{m\zeta}$ and β, are left which can be tuned to achieve a close match between the pre-specified conduction velocity, C^v_ζ, and the velocity, $\bar{C}^v_\zeta$, predicted by the simulation.

In ventricular models C^v is orthotropic, thus necessitating to find parameters along each of the three eigenaxes. Among the two parameters available for fitting $\bar{C}^v_\zeta$, β scales conduction velocity isotropically along all axes ζ. Using (5) and (2), and keeping β at a chosen default value, one can find unique monodomain conductivities along all axes ζ, which yield the prescribed conduction velocities, C^v_ζ, by iteratively refining conductivities $\sigma_{m\zeta}$ based on C^v_ζ measured in simple 1D cable simulations. The iterative update scheme we propose is given as

Algorithm 1 Iterative conductivity tuning

```
i=0
σ_mζ [i] = σ^0_mζ
repeat
C̄^v_ζ[i] ← Simulation
σ_mζ[i+1] = σ_mζ[i].(C^v_ζ / C̄^v_ζ[i])^2
i=i+1
until ‖ C̄^v_ζ[i−1] − C^v_ζ ‖ /C^v_ζ > stop_tol
```

where σ^0_m is an arbitrary initial guess which is used during the first simulation run.

2.4. Compensation of discretization effects

When using bidomain parameters as chosen based on the proposed strategy, C^v must be independent of the

choice of spatial discretization, $\Delta\zeta$. The influence of $\Delta\zeta$ is studied in a 1D strand model of $1cm$ length in which $\Delta\zeta$ is varied between $1\mu m$ up to $400\mu m$. $\sigma_{m\zeta}$ is iteratively tuned at the $1\mu m$ grid to yield a C^v of $0.6m/s$, $0.4m/s$ and $0.2m/s$, respectively. At each discretization and for each $\sigma_{m\zeta}$, propagation is initiated at the left hand side end of the cable and $\bar{C}^v$ as well as the spatial extent of the wavefront, ΔX_ζ, is measured at its center. Plots are constructed to show $\bar{C}^v$ as a function of $\Delta\zeta$. Finally, each simulation is repeated, replacing $\sigma_{m\zeta}$, as fitted for the $1\mu m$ grid, by $\bar{\sigma}_{m\zeta}$, as computed by the iterative tuning loop described in algorithm 1.

2.5. Obtaining bidomain conductivities

Although anisotropy ratios, on mathematical grounds, are of rather minor relevance when simulating impulse propagation in tissue, when the stimulation of cardiac tissue via externally applied electric fields are studied, anisotropy ratios play a prominent role. For this case additional constraints are required to adjust the anisotropy ratio α while keeping conduction velocities unaltered. Using the definition $\alpha_\zeta = \frac{\sigma_{i\zeta}}{\sigma_{e\zeta}}$ to characterize differences in conductivities between intracellular and extracellular space along an axis ζ, and $\varepsilon_{i\zeta} = \frac{\sigma_{il}}{\sigma_{i\zeta}}, \varepsilon_{e\zeta} = \frac{\sigma_{el}}{\sigma_{e\zeta}}$ to characterize differences in conductivity within the same space, but between an axis $\zeta = t|n$ relative to the longitudinal axis, $\zeta = l$, we may express the anisotropy ratio $\varepsilon_{l,\zeta}$ as

$$\varepsilon_{l,\zeta} = \frac{\varepsilon_{i\zeta}}{\varepsilon_{e\zeta}} = \frac{\alpha_l}{\alpha_\zeta}.$$

Note that we present quantities relative to the longitudinal axes where ζ is then either t or n.

To determine the four individual bidomain conductivities we chose the desired anisotropy ratio ε_{lt} and the longitudinal conductivity σ_{il} as these quantities show the smallest variance in the literature [3–5]. Using these constraints the bidomain conductivities are determined using (3) as

$$\sigma^*_{ml} = \frac{1}{1+\alpha_l}\sigma'_{il},\ \sigma^*_{m\zeta} = \frac{1}{1+\frac{\alpha_l}{\alpha'_\zeta}}\frac{1}{\alpha_{i\zeta}}\sigma'_{il} \tag{7}$$

where * denotes quantities which were determined by iterative simulations, as outlined in Algorithm 1, and primed quantities are chosen values. Solving equations (7) for a_l and α_ζ allows to find the bidomain conductivities

$$\sigma_{il} = 1\cdot\sigma'_{il} \qquad \sigma_{el} = \frac{1}{a_l}\cdot\sigma'_{il} \tag{8}$$

$$\sigma_{i\zeta} = \frac{1}{\alpha_{i\zeta}}\cdot\sigma'_{il} \qquad \sigma_{e\zeta} = \frac{\alpha'_\zeta}{\alpha_{i\zeta}a_l}\cdot\sigma'_{il} \tag{9}$$

In the transversely orthotropic case, Eq. (7) is solved with $\zeta = t$, whereas in the orthotropic case Eq. (7) is solved once more with $\zeta = n$.

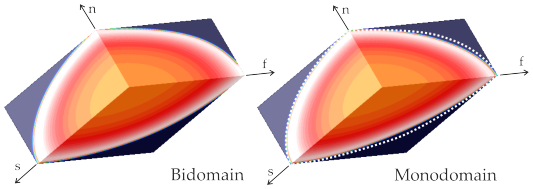

Figure 1. Comparison between bidomain and an equivalent monodomain model in a 3D slab model. White dashed lines in the Monodomain panel indicate position of the wavefront in a bidomain setting for the same instant in time. f, s and n are orthotropic main axes.

3. Results

3.1. Monodomain-bidomain equivalence

While the exact equivalence between bidomain and monodomain model using harmonic mean conductivities does not hold in 3D, along the principal eigenaxes the agreement between the models is quite good (Fig. 1). This close agreement suggests that the equivalent monodomain model can be used within the Algorithm 1, yielding a set of conductivities which enforce the prescribed C^v also when using a 3D bidomain model.

3.2. Conduction velocity parameterization

Using the iterative algorithm 1, conductivities were chosen to arrive at the prescribed velocities of C^v_ζ =0.6, 0.4 and $0.2m/s$ for planar wave fronts traveling along the axes $\zeta = f, s, n$, respectively. Fig. 2A shows how simulated velocities $\bar{C}^v_\zeta$ are affected when increasing grid resolution $\Delta\zeta$ stepwise from $1\mu m$ to $400\mu m$. Numerical errors of 5% incurred at different spatial resolutions of $\Delta\zeta$ =275μm, 180μm and 90μm for C^v_f, C^v_s and C^v_n, respectively. As expected, scaling of simulated velocities with the prescribed velocity, i.e. $\epsilon_v = \bar{C}^v_\zeta/\bar{C}^v_\zeta/$, reveals that spatial discretization errors are mainly governed by the ratio $\Delta\zeta/\Delta X_\zeta$ (Fig. 2B). Convergence experiments were repeated for C^v_f =0.6m/s and all discretizations $\Delta\zeta$, but equations were re-parameterized using the automatic parameterization strategy (APS) as described in algorithm 1. While conductivities varied in the range between -6 to +24%, wave fronts propagated with the exact prescribed C^v, independently of $\Delta\zeta$.

3.3. Choice of individual conductivities

Considering a transversely isotropic scenario, the analytic expressions 9 were used to obtain individual conductivities given three different anisotropy ratios: 1) unequal anisotropy, with $\varepsilon_{l,t} = 4.5$, 2) equal anisotropy, with $\varepsilon_{l,t} = 1$, and 3) inverse anisotropy, with $\varepsilon_{l,t} = 1/4.5$. The

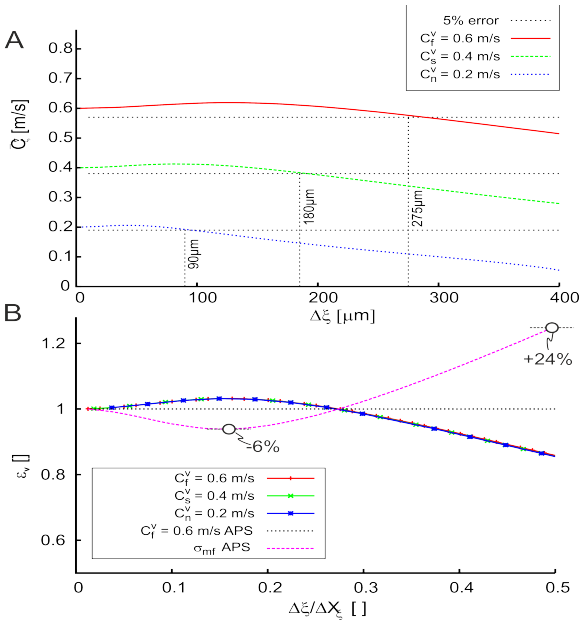

Figure 2. A) Influence of spatial discretization $\Delta\zeta$ upon predicted conduction velocities for propagation along the axes f, s and n. B) Deviations in relative velocity, $\epsilon_v = \bar{C}_\zeta^v / C_\zeta^v$ depend on the ratio $\Delta\zeta$ to spatial extent of wave front, ΔX_ζ. Using APS, predicted C^v (black dotted trace) is independent of $\Delta\zeta$, at the cost of minor variations of the chosen conductivity value, σ_{mf} (pink trace)

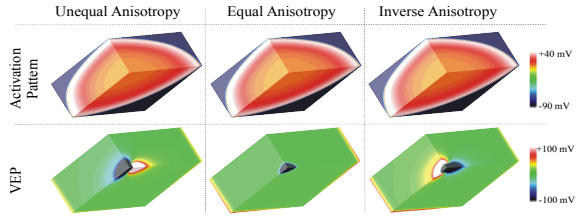

Figure 3. Anisotropy ratios are chosen without affecting conduction velocity. Upper panels show activation sequences for three different anisotropy ratios. Lower panels show the induced VEPs in response to a strong hyperpolarizing point stimulus for the same given anisotropy ratios.

propagation patterns and the virtual electrode propagation (VEP) are shown in Fig. 3. Note that during normal propagation differences in anisotropy ratio do not manifest in the activation patterns. However, a different VEP is induced for each anisotropy ratio.

4. Discussion

In this study an iterative parameterization strategy is proposed that allows to find appropriate tissue conductivities which result then in the prescribed C_ζ^v along the orthotropic eigenaxes f, s and n of the tissue, as well as prescribed anisotropy ratios. Computationally cheap 1D equivalent monodomain models can be used in the parameterization loop to determine conductivities which are also suited for bidomain simulations. It is worth noting that parameter variations due to the automatic parameterization strategy, between -6% up to +24% around the nominal values, are well below the experimentally measured variability. The effectiveness of the methods is demonstrated for spatial discretizations of up to $400\mu m$, however, for even coarser discretizations this may not be the case anymore. However, in line with the current trend towards anatomically detailed ventricular models, finer spatial resolution down to average discretizations of around $\approx 100\mu m$ are becoming standard to resolve geometric details. With such finer spatial steps $\Delta\zeta$, relative discretization of wave fronts $\Delta\zeta/\Delta X_\zeta$ is less than 0.3 and necessary modifications of conductivity values are below 6%.

Acknowledgment

This research is supported by Austrian Science Fund FWF grant F3210-N18.

References

[1] Prassl AJ, Kickinger F, Ahammer H, et al. Automatically Generated, Anatomically Accurate Meshes for Cardiac Electrophysiology Problems. IEEE Trans Biomed Eng 2008;.

[2] Plank G, Burton RAB, Hales P, et al. Generation of histo-anatomically representative models of the individual heart: tools and application. Philos Transact A Math Phys Eng Sci Jun 2009;367(1896):2257–2292.

[3] Clerc L. Directional Differences of Impulse Spread in Trabecular Muscle from Mammalian Heart. J Physiol 1976; 255:335–346.

[4] Roberts DE, Hersh LT, Scher AM. Influence of cardiac fiber orientation on wavefront voltage, conduction velocity, and tissue resistivity in the dog. Circ Res 1979;44(5):701–12.

[5] Roberts DE, Scher AM. Effect of tissue anisotropy on extracellular potential fields in canine myocardium in situ. Circulation Research 1982;50:342–51.

Address for correspondence:

Gernot Plank
Medical University of Graz, Institute of Biophysics
Harrachgasse 21/IV
A-8010, Graz, Austria
gernot.plank@medunigraz.at